ADBA
Computers and Electronics in Medicine
Cutting-Edge Scientific Solutions

e-ISSN: 3023-8609
RESEARCH ARTICLE
Vol.3 / No.1 / 2026 / pp.99-108
https://doi.org/10.69882/adba.cem.20260112

Adaptive–Scaled Digital Watermarking in Color Medical Imaging

İrem Özmen [α,1], **Zeynep Çetinkaya** [α,2], **Fahrettin Horasan** [α,3], **Fatih Varçın** [β,4] **and Shaobo He** [*,5]

[α]Department of Computer Engineering, Kırıkkale University, Kırıkkale, Türkiye, [β]Department of Computer Engineering, Sakarya University of Applied Sciences, Sakarya, Türkiye, [*]School of Automation and Electronic Information, Xiangtan University, Xiangtan, 411105, China.

ABSTRACT Nowadays digital environment, the rapid duplication and unauthorized use of color images shared online have led to increasing concerns regarding copyright infringement and data security. Therefore, the development of effective and robust methods for protecting digital content has become critically important. In this study, an integrated digital watermarking method is proposed to ensure copyright protection and data security for both color and medical images. In the proposed approach, watermark embedding is performed by jointly applying Discrete Wavelet Transform (DWT) and Singular Value Decomposition (SVD) on the blue (B) color channel of the cover image. The watermark image is preprocessed using a dimension reduction technique and optimized through the Grey Wolf Optimization (GWO) algorithm. The optimized watermark is then embedded into the cover image, and inverse transformations are applied to obtain the watermarked image. The performance of the proposed algorithm is evaluated on standard test images under various attack scenarios. Imperceptibility is assessed using Peak Signal-to-Noise Ratio (PSNR) and Structural Similarity Index (SSIM), while robustness is measured using the Normalized Correlation (NC) and Bit Error Rate (BER) metrics. Experimental results demonstrate that the proposed method achieves high imperceptibility and successfully preserves watermark information under different attacks. Comparisons with related studies in the literature indicate that the proposed approach is competitive and, in some cases, superior in terms of both imperceptibility and robustness. Consequently, the proposed method provides an effective and reliable digital watermarking solution for color images.

KEYWORDS
Data hiding
Color image
Medical image watermarking
Dimension reduction

INTRODUCTION

With the advancement of the technological era, the increasing volume of digital data has made the storage, transmission, and confidentiality of this data more critical (Gull and Parah 2024; Awasthi *et al.* 2024). This situation has led to a growing importance of security systems developed to ensure data security, which are generally classified into data encryption and data hiding techniques (Çelik and Doğan 2021). Cryptography, a subfield of data encryption, is a method that encrypts content to prevent it from being read by unauthorized parties and ensures that it is accessible only to authorized users (Çelik and Yalçın 2023; Çelik and Doğan 2021). Steganography, as a subcategory of data hiding, aims to preserve data confidentiality by concealing the very existence of the data (Awasthi *et al.* 2024; Çelik and Doğan 2021).

In digital image watermarking, copyright protection allows the verification of content ownership by embedding a hidden watermark into an image (Awasthi *et al.* 2024; Çelik and Doğan 2021). During the watermarking process applied to digital data, the modifications introduced into the data must remain imperceptible to third parties. In other words, the impact of the watermarking process on the original digital data should be minimized as much as possible (Nawaz *et al.* 2025). From this perspective, digital watermarking provides an effective solution for ensuring data security (Wang *et al.* 2023). The digital watermarking process consists of two main stages: watermark embedding and watermark extraction (Mamuti 2019). In the watermark embedding stage, the watermark information is embedded into the cover signal (Awasthi *et al.* 2024; Yağcıoğlu and Sondaş 2021), while in the extraction and verification stage, the watermark is retrieved by the receiver and the verification process is performed. The stages of the digital watermarking process are illustrated in Figure 1.

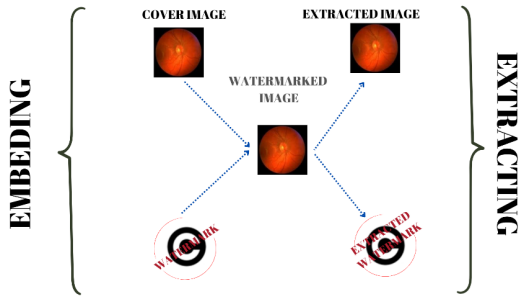

Figure 1 Watermarking scheme (embedding and extraction)

Watermarking methods are classified according to various criteria in order to meet different application requirements, and this study focuses on approaches used for color images (Wang *et al.*

Manuscript received: 14 October 2025,
Revised: 7 January 2026,
Accepted: 7 January 2026.

[1]irem_ozmen@kku.edu.tr
[2]zeynepcetinkaya@kku.edu.tr
[3]fhorasan@kku.edu.tr (**Corresponding author**)
[4]fatihvarcin@subu.edu.tr
[5]heshaobo@xtu.edu.cn

2023; Mahto and Singh 2021; Sharma *et al.* 2023). This classification is based on the type of cover signal, watermark perceptibility, embedding domain, robustness, and data extraction method (Nawaz *et al.* 2025; Mahto and Singh 2021).

The first criterion used in the classification of watermarking methods is the type of the cover signal. Different signal types such as text, image, audio, and video can be used as cover signals in the watermarking process (Awasthi *et al.* 2024; Mahto and Singh 2021). Another classification criterion is whether the watermark is perceptible to the human visual system. In this context, watermarking methods are divided into two groups: visible and invisible watermarking (Awasthi *et al.* 2024; Mahto and Singh 2021; Sharma *et al.* 2023). Invisible watermarks are generally used in applications such as copyright protection, image authentication, and privacy protection (Mahto and Singh 2021).

The domain in which the watermarking process is performed is also an important classification criterion (Wang *et al.* 2023; Mahto and Singh 2021). A watermark can be embedded either in the spatial domain or in the transform domain of the cover signal (Hu 2024; Sharma *et al.* 2023). In the Least Significant Bit (LSB) technique, which is one of the spatial domain methods, watermark bits are stored in the least significant bits of the pixels of the carrier image (Gull and Parah 2024; Wang *et al.* 2016). In transform-domain methods, the image is represented using specific mathematical transformations; examples include techniques based on DWT, DCT, and SVD (Hu 2024; Sharma *et al.* 2023; Wang *et al.* 2016). The ability of transform-domain methods to effectively exploit the principles of the human visual system and visual perception characteristics has made them highly popular (Hu 2024). In line with these advantages, this study proposes a watermarking method based on transform-domain techniques.

Watermarking techniques are also classified according to their robustness against external attacks. In this context, they are generally categorized into three main groups: fragile, semi-fragile, and robust watermarking methods (Mahto and Singh 2021; Anand and Singh 2021; Singh *et al.* 2023). Robust watermarks exhibit resistance to both intentional and unintentional modifications applied to the image (Awasthi *et al.* 2024). In contrast, fragile watermarks are easily degraded even by minor alterations. Semi-fragile watermarking methods provide resistance to certain types of attacks while enabling the detection of content manipulations (Zainol *et al.* 2021; Sharma *et al.* 2024). Finally, watermarking systems are classified into three groups blind, semi-blind, and non-blind based on the information required during the watermark extraction process (Awasthi *et al.* 2024; Sharma *et al.* 2023). In blind watermarking methods, the original image is not required at the extraction stage; semi-blind watermarking methods require only the original watermark information, whereas non-blind watermarking methods require both the cover image and the watermark information (Awasthi *et al.* 2024; Sharma *et al.* 2023; Zainol *et al.* 2021).

There are three fundamental properties that determine the performance of digital watermarking systems: imperceptibility, robustness, and capacity. Imperceptibility refers to the similarity between the cover image and the watermarked image obtained after the watermarking process. In other words, it indicates the level of distortion introduced into the cover image by the watermark embedding operation . Robustness is defined as the similarity between the original watermark image and the watermark extracted from the watermarked image, and it represents the degree of degradation affecting the watermark during the watermarking process (Awasthi *et al.* 2024; Hu 2024; Zainol *et al.* 2021). Capacity denotes the amount of watermark data that can be embedded into the cover image. Establishing an appropriate balance among these parameters is of great importance for the overall performance of watermarking systems (Hu 2024).

In watermarking schemes, the relationship among robustness, imperceptibility, and capacity follows a trade-off structure (Begum and Uddin 2020). For instance, as the data payload increases, i.e., as capacity is enhanced, the robustness of the watermark decreases while its perceptibility increases. Similarly, improving imperceptibility may lead to a reduction in both robustness and capacity. Maintaining all parameters at optimal levels within this trade-off triangle is one of the primary objectives of digital watermarking systems (Begum and Uddin 2020; Qasim *et al.* 2018). These trade-off components are illustrated in Figure 2.

Figure 2 Trade-off components (imperceptibility, robustness, and capacity)

In watermarking methods, not only the structure of the watermark image but also the type of the cover (host) image is an important classification criterion that affects the design and performance of the algorithm. While cover images may be grayscale or color, watermark images can be used in binary, grayscale, or color formats depending on the application (Wang *et al.* 2023; Sharma *et al.* 2023). These different data structures of the cover and watermark images directly influence performance metrics such as capacity, imperceptibility, and robustness of watermarking methods.

Color cover images are represented in the RGB color space and have a three-dimensional matrix structure consisting of rows, columns, and color channels. Within this structure, each layer corresponds to one of the red (R), green (G), and blue (B) color components. Each color channel can be treated as a grayscale image, and the watermarking process can be applied separately to these channels (Hu 2024; Mamuti 2019). This multi-channel structure enables higher data embedding capacity during the watermarking process (Wang *et al.* 2023; Hu 2024).

The watermark image, on the other hand, can be selected as binary, grayscale, or color depending on the application. Embedding strategies and extraction methods vary according to the data structure of the watermark (Wang *et al.* 2023; Sharma *et al.* 2023). In this study, color images are preferred as cover images, while a grayscale image is used as the watermark. This choice aims to exploit the capacity advantage provided by color cover images while establishing a balanced structure between imperceptibility and robustness through the use of a grayscale watermark.

Performance evaluation in watermarking methods is generally carried out based on imperceptibility and robustness criteria (Awasthi *et al.* 2024). To assess the imperceptibility performance of watermarking schemes, Peak Signal-to-Noise Ratio (PSNR) and

Structural Similarity Index (SSIM) metrics are widely used for image quality and similarity analysis. For robustness evaluation, the Normalized Correlation (NC) metric is employed to measure the similarity between the extracted watermark and the original watermark, while the Bit Error Rate (BER) metric is used to assess the degree of robustness (Karmouni *et al.* 2024; Çelik and Yalçın 2023; Melman and Evsutin 2023). The PSNR metric is calculated using the following Equation (1).

$$\mathrm{PSNR}(H, H_w) = 10 \log_{10} \left(\frac{\mathrm{Max}_H^2}{\mathrm{MSE}} \right) \tag{1}$$

Here, H denotes the cover image, while Hw represents the watermarked image. The Mean Squared Error (MSE) represents the average pixel-wise error between the cover and watermarked images (Eltoukhy *et al.* 2023). MSE is defined by Equation (2):

$$\mathrm{MSE} = \frac{1}{N^2} \sum_{x=1}^{n} \sum_{y=1}^{n} [H(x,y) - H_w(x,y)]^2 \tag{2}$$

The SSIM, which is a structural similarity measure, is defined by Equation (3):

$$\mathrm{SSIM}(H, H_w) = \frac{(2\mu_H \mu_{H_w} + C_1)(2\sigma_{HH_w} + C_2)}{(\mu_H^2 + \mu_{H_w}^2 + C_1)(\sigma_H^2 + \sigma_{H_w}^2 + C_2)} \tag{3}$$

Here, μ_H and μ_{H_w} denote the local mean values of the cover image H and the watermarked image H_w, respectively, while σ_H and σ_{H_w} represent their corresponding standard deviations. The constants C_1 and C_2 are introduced to ensure numerical stability during computation. For an ideally imperceptible watermarking algorithm, the SSIM value is expected to be close to 1 (Horasan *et al.* 2019; Mousavi *et al.* 2014).

To evaluate robustness in watermarking schemes, the watermarked image is subjected to various potential attacks during testing (Mousavi *et al.* 2014). These attacks are generally classified as geometric and conventional attacks. Commonly applied attack types include rotation, cropping, copy–paste, deletion, median filtering, JPEG compression, salt-and-pepper noise, and Gaussian filtering operations (Li *et al.* 2023; Khare and Srivastava 2021; Horasan *et al.* 2019).

The NC metric, which is used for robustness evaluation, is defined by Equation (4):

$$\mathrm{NC} = \frac{\sum_{i=1}^{P} \sum_{j=1}^{Q} w(i,j)\, w'(i,j)}{\sum_{i=1}^{P} \sum_{j=1}^{Q} [w(i,j)]^2} \tag{4}$$

In this equation, $w(i,j)$ represents the original watermark image, while $w'(i,j)$ denotes the extracted watermark image (Mohanarathinam *et al.* 2020; Anand and Singh 2021). An NC value greater than 0.75 under attack conditions and close to 1 under ideal conditions is generally expected. As the NC value approaches unity, the watermarking method is regarded as robust and resilient (Yurttakal and Horasan 2022; Priyadarshini and Naik 2024).

The BER metric, which is used to evaluate robustness, represents the ratio of incorrectly extracted bits to the total number of embedded bits. BER values range between 0 and 1, where a value of 0 indicates error-free extraction [38]. BER is defined by Equation (5):

$$\mathrm{BER} = \frac{\text{Number of Errors}}{\text{Total Number of Transmitted Bits}} \tag{5}$$

LITERATURE REVIEW

The rapid production and sharing of visual data in digital environments have led to increasing issues related to copyright infringement and unauthorized use. In this context, digital image watermarking has emerged as an effective solution for ownership verification, preservation of content integrity, and prevention of unauthorized copying. Although early studies primarily focused on grayscale images, the widespread use of color images in real-world applications has necessitated the adaptation of watermarking methods to multi-channel and more complex structures. The presence of multiple channels in color images offers the potential to increase watermark embedding capacity, while also introducing new challenges due to inter-channel correlations and compression processes.

Studies in the field of color image watermarking have predominantly focused on classical transform-domain-based approaches. In this regard, Wang *et al.* (2023) proposed a blind color image watermarking method using mid-frequency coefficients in the two-dimensional Discrete Cosine Transform (2D-DCT) domain. To enhance watermark security, a two-stage encryption process based on affine transformation and Arnold transform was applied. In addition, imperceptibility and robustness were improved by employing variable embedding coefficients across different blocks and layers. Although such DCT-based methods provide high visual quality, a significant portion of approaches operating in the RGB color space do not explicitly address the effects of color space transformation and quantization applied during the JPEG compression process. This limitation may lead to notable performance degradation of RGB-based watermarks, particularly under JPEG attacks.

The neglect of spectral relationships among RGB channels has emerged as one of the fundamental weaknesses of color image watermarking methods in the literature. Addressing this issue, Hu (2024) demonstrated that the conversion to the YCbCr color space and the quantization of chroma components during the JPEG compression process have destructive effects on watermark information embedded in RGB channels. To mitigate this problem, the proposed synergistic compensation (SC) approach aims to enhance JPEG robustness by suppressing quantization errors in channels where the watermark is not embedded.

Other studies aiming to model inter-channel relationships in a more holistic manner have focused on quaternion-based approaches. Wang *et al.* (2025) proposed a watermarking method that preserves linear correlations among RGB channels by employing a split quaternion matrix model and double-layer singular value decomposition. Similarly, Wang *et al.* (2013) introduced a blind watermarking method based on the quaternion Fourier transform, targeting high robustness against both color-based attacks and geometric distortions. Although such methods provide strong robustness, they involve practical limitations such as increased computational cost and additional information requirements.

More recent studies in the literature have emphasized optimization-based and hybrid-domain approaches to improve the imperceptibility–robustness trade-off. Sharma *et al.* (2023) and Sahir *et al.* (2025) optimized scaling factors in DWT–SVD and DWT–HD–SVD frameworks, respectively, using the Artificial Bee Colony (ABC) algorithm, thereby enhancing both visual quality and robustness against attacks. Agarwal and Singh (2022) employed a genetic algorithm in the DCT domain to select optimal pixel groups, achieving notable improvements in PSNR and NCC values, particularly across RGB channels. Ahmadi *et al.* (2021) proposed a blind dual watermarking approach based on

DWT–SVD and Particle Swarm Optimization (PSO), addressing both copyright protection and integrity authentication within a unified framework; robust watermarking performed specifically on the blue channel resulted in high capacity and robustness.

Among approaches focusing on lower computational cost, Su and Chen (2018) proposed a blind color image watermarking method that directly utilizes DC coefficients in the spatial domain instead of the transform domain, achieving satisfactory robustness against JPEG compression and noise attacks. This method stands out in terms of processing speed and implementation simplicity. Roy and Pal (2019) introduced a DWT–SVD-based approach relying solely on the luminance component in the YCbCr color space; although the method demonstrates robustness under various attacks, its non-blind structure and single-channel utilization limit its capacity. In the context of medical image security, Eltoukhy *et al.* (2023) developed a watermarking method based on Slant–SVD–QFT transforms combined with one-time pad (OTP) encryption, providing very high visual quality and security. Finally, Su *et al.* (2024) presented a low-latency, high-security, and fully blind fusion-domain watermarking scheme using graph-based transformation and PSO.mOverall, a review of the literature reveals that the field of color image watermarking has witnessed a wide diversity of methods and significant advancements, ranging from classical transform-domain approaches to quaternion-based models, and from heuristic optimization algorithms to graph-based and learning-assisted techniques. These studies offer various advantages in terms of imperceptibility, robustness, security, and computational efficiency.

However, it is noteworthy that the effects of attacks originating from color space transformations and quantization processes such as those introduced by JPEG compression are often addressed indirectly or treated as secondary issues in many studies, particularly in RGB-based methods. Therefore, approaches that explicitly consider the interaction between color space conversion and compression processes provide a complementary and strengthening perspective to existing methods.

THEORICAL BACKGROUND

Discrete Wavelet Transform (DWT)

The DWT is an effective signal processing technique that enables multilevel analysis by decomposing images into their frequency components. Through the LL, LH, HL, and HH sub-bands obtained after applying DWT, the fundamental structural information and detailed components of an image can be separated (Wang *et al.* 2016; Othman and Zeebaree 2020). The high time–frequency localization capability provided by DWT allows the watermark to be embedded efficiently without significantly degrading image quality. Moreover, the ability to extract the watermark without requiring the original image makes DWT a suitable method for applications such as compression and noise reduction (Othman and Zeebaree 2020).

In DWT-based watermarking approaches for color images, the image is first decomposed into RGB or YCbCr color spaces, and DWT is applied separately to each color channel to obtain the corresponding sub-bands. By selecting appropriate sub-bands for watermark embedding, visual quality can be preserved while robustness against signal-processing-based attacks is enhanced (Karmouni *et al.* 2024). The DWT-based approach for color images is schematically illustrated in Figure 3.

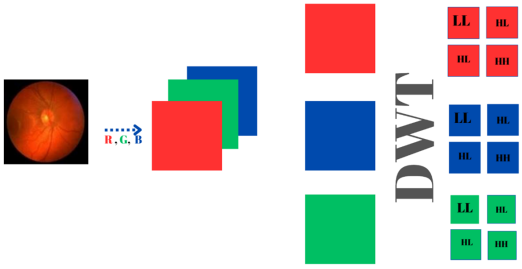

Figure 3 DWT-based approach for color images

Singular Value Decomposition (SVD)

SVD is a powerful linear algebra technique that is widely used in image processing and, in particular, in digital watermarking due to its ability to preserve visual quality and provide robustness against various distortions [19]. SVD decomposes an image matrix into three matrices (U, S, V^T) where the singular values in S capture the intrinsic properties of the image and exhibit high stability under common image processing operations (Mohanarathinam *et al.* 2020; Zainol *et al.* 2021).

In the literature, SVD is commonly combined with the DWT in adaptive watermarking algorithms that allow watermark embedding in both low- and high-frequency components. Such approaches contribute to the development of robust watermarking systems capable of withstanding attacks such as contrast and brightness adjustments, cropping, and noise addition (Mohanarathinam *et al.* 2020). The application of SVD on images is illustrated in Figure 4.

Figure 4 Application of Singular Value Decomposition

Dimension Reduction

Dimension reduction is an approach that aims to obtain a more compact representation that preserves the essential structure of the data by eliminating components that are considered noise or do not carry meaningful information in large datasets. This process not only reduces computational cost but also increases data processing speed and enhances system robustness by suppressing noise present in the signal. As a result, more meaningful relationships can be revealed, and in applications such as watermarking, the imperceptibility performance can be improved (Yurttakal and Horasan 2022; Horasan *et al.* 2019; Çetinkaya and Horasan 2025). The general structure of the dimension reduction approach is illustrated in Figure 5.

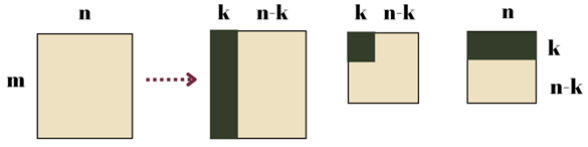

Figure 5 Dimension Reduction

Optimization Algorithm

Optimization is a process that aims to obtain the best (optimal) value of an objective function defined under certain constraints (Melman and Evsutin 2023). In this study, Grey Wolf Optimization (GWO) is examined and applied. GWO is an optimization algorithm inspired by the social hierarchy and hunting behavior of grey wolf packs, proposed by Mirjalili et all. (Seyedali and Andrew 2014). In this method, candidate solutions are represented by alpha, beta, delta, and omega wolves, and the search process is guided according to this hierarchical structure (Mirjalili 2015; Seyedali and Andrew 2014). The position update mechanism, which models the encircling and attacking phases of prey, together with a linearly decreasing control parameter, enables the algorithm to gradually transition from the exploration phase to the exploitation phase (Rodríguez *et al.* 2017; Seyedali and Andrew 2014).

MATERIAL AND METHOD

Embedding Process

In this study, color images in RGB format were selected as cover images, and these images were decomposed into three color channels: red (R), green (G), and blue (B). The digital watermarking process was performed solely on the B channel, and the matrix corresponding to this channel was obtained. The DWT was applied to the obtained B matrix, and among the subbands obtained from the transformation, the low-frequency LL band was selected for processing. The SVD algorithm was applied to the LL band to obtain a singular value matrix from this band. Similarly, the rank-k SVD algorithm was applied to the data to be used as the watermark for dimension reduction, and the singular value matrix of the watermark was computed. These two singular value matrices obtained from the cover image and the watermark data were summed prior to the merging operation to form a new singular value matrix. The resulting new singular values were reconstructed using the inverse SVD process.

The Inverse DWT was applied to the LL band obtained from this process to yield the B channel matrix containing the digital watermark. In the final stage, the original R and G channels were combined with the watermarked B channel to successfully generate the watermarked color image. The stages of the DWT–SVD based watermark embedding process performed on the B channel of the cover image are schematically illustrated in Figure 6.

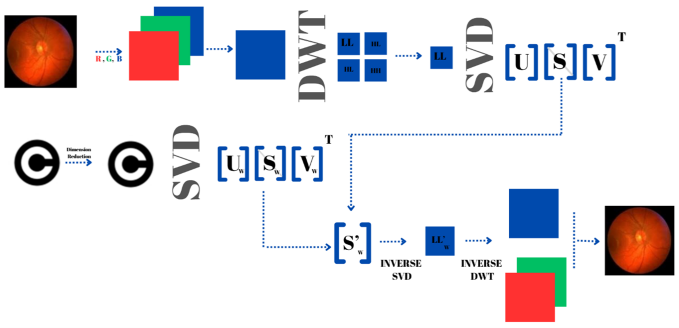

Figure 6 Embedding Process

Extraction Process

After obtaining the watermarked image, the image was decomposed into RGB color channels, and all operations were performed solely on the B channel. The DWT was applied to this channel, decomposing the image into four subbands: LL, LH, HL, and HH.

SVD was applied to the low-frequency LL band of the watermarked image, and the corresponding singular value matrix was obtained as a result of this operation. For watermark extraction, the singular value matrix of the original cover image was subtracted from the singular value matrix obtained from the watermarked image, thereby isolating the singular values corresponding exclusively to the embedded watermark.

These isolated singular values were combined with the other two SVD matrices of the watermark obtained during the embedding stage, and the watermark image was reconstructed using the Inverse SVD method. As a result of this process, the watermark image was successfully retrieved. The extracted watermark image has the same dimensions as the dimension reduced watermark used in the embedding stage. The overall workflow of the proposed watermark extraction process is illustrated in Figure 7.

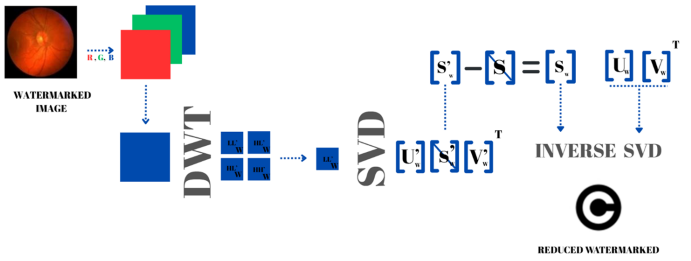

Figure 7 Extraction Process

Optimization Process

In this study, an optimization problem was defined to determine the optimal values of the parameters used in the RGB multi-level DWT–SVD based watermarking method. The optimization process aims to achieve a balance between the robustness and imperceptibility metrics obtained under different attack scenarios.

The optimization problem involves two fundamental decision variables: k, representing the rank value employed in the SVD of the watermark, and α, denoting the scaling coefficient used to embed the watermark into the singular values of the cover image.

When the constraints are examined in detail:

- **Rank (k) Constraint:** Given that the watermark image has dimensions $h_w \times w_w$, the maximum meaningful rank value is defined in Equation (6).

$$k_{\max} = \min(h_w, w_w) \tag{6}$$

To prevent the adverse effects of excessively small or excessively large rank values, it has been constrained within the range specified in Equation 7.

$$0.1\,k_{\max} \leq k \leq 0.75\,k_{\max} \tag{7}$$

This constraint prevents both excessive reduction of the watermark and overly aggressive embedding.

- **Scaling Coefficient (α) Constraint**: This controls the effect of the watermark on the cover image. This parameter is defined in the continuous interval in Equation 8.

$$\alpha_{\min} \leq \alpha \leq \alpha_{\max} \tag{8}$$

This range has been determined experimentally to provide a reasonable balance between imperceptibility and robustness.

Each candidate solution (k, α) was evaluated using NC, BER, SSIM and PSNR metrics under multiple attack scenarios. The results of these metrics reflect both the extractability of the watermark and the perceptual quality of the cover image. When these metrics are examined:

- PSNR Normalization: Since the PSNR value is measured in dB, it has been normalized to be evaluated on the same scale as the other metrics, as given in Equation 9.

$$\text{normalizedPSNR} = \begin{cases} 1, & \text{PSNR} \geq 37, \\ \dfrac{\text{PSNR}}{37}, & \text{PSNR} < 37. \end{cases} \tag{9}$$

  This threshold was determined based on the 37 dB reference, which is widely accepted in the literature for high perceptual quality.
- Attack-Based Average Performance: For a candidate solution (k, α), the averages of the metrics obtained under all attack scenarios are defined as follows Equations 10-13, N denotes the total number of attacks employed.

$$\overline{\text{NC}} = \frac{1}{N}\sum_{i=1}^{N} \text{NC}_i \tag{10}$$

$$\overline{\text{invBER}} = \frac{1}{N}\sum_{i=1}^{N} (1 - \text{BER}_i) \tag{11}$$

$$\overline{\text{SSIM}} = \frac{1}{N}\sum_{i=1}^{N} \text{SSIM}_i \tag{12}$$

$$\overline{\text{PSNR}}_{\text{norm}} = \frac{1}{N}\sum_{i=1}^{N} \text{PSNR}_{\text{norm},i} \tag{13}$$

In this study, the fitness function is defined in Equation 14 to minimize the difference between the average robustness and imperceptibility metrics across all attack scenarios

$$\text{fit}(k, \alpha) = \frac{1}{N}\sum_{i=1}^{N} |\text{NC}_i + \text{invBER}_i - \text{SSIM}_i - \text{normalizedPSNR}_i| \tag{14}$$

The primary objective of this formulation is to ensure that the terms representing robustness, $NC_i + invBER_i$ and those representing imperceptibility, $SSIM_i + normalizedPSNR_i$ are as close to each other as possible. The optimization problem under the defined fitness function and constraints is expressed in Equation 15 as follows.

$$(k^*, \alpha^*) = \arg\min_{k,\alpha} \text{fit}(k, \alpha) \tag{15}$$

Through this structure, the optimization process is directed toward producing a balanced solution between robustness and imperceptibility, rather than excessively optimizing a single metric.

EXPERIMENTAL RESULTS

To evaluate the performance of the proposed watermarking algorithm, both medical and standard benchmark color images were employed as cover images. As illustrated in Figure 1(a), the selected cover images include Melanoma, Cerebral, Retinal Fundus, Baboon, and Peppers, which are widely used benchmark images in digital watermarking studies. All cover images have a spatial resolution of 512 × 512 pixels.

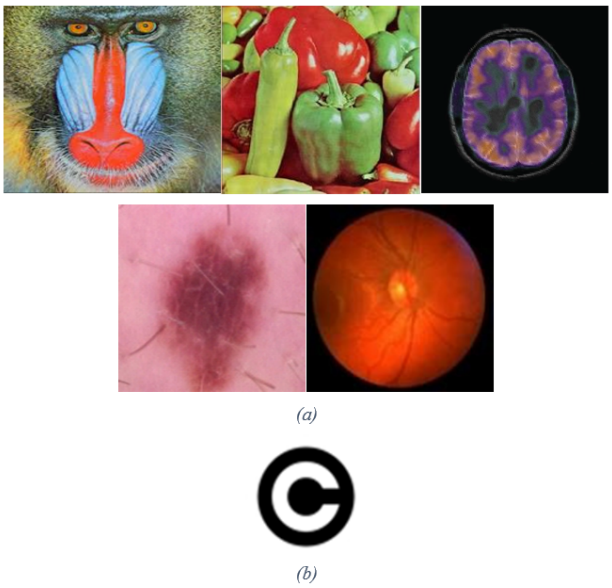

(a)

(b)

Figure 8 (a) Color Cover Images [Baboon, Peppers, Cerebral, Melanoma, Retinal Fundus] (b) Watermark [copyright]

Table 1 presents the optimal k parameter and the optimal α values obtained for different cover images and watermark sizes. When all cover images are considered, it is observed that the optimal k value decreases as the watermark size becomes smaller. This indicates that the rank parameter is directly dependent on the watermark dimensions. The optimal α parameter, namely the watermark embedding coefficient, shows an increasing trend as the watermark size decreases. This result indicates that a stronger embedding operation is required to maintain robustness when smaller watermarks are used. The obtained findings clearly demonstrate the drawbacks of using fixed parameter values and highlight the necessity of optimization-based parameter selection.

To evaluate the performance of the proposed DWT–SVD-based watermarking method using the optimized parameters, NC, BER, SSIM, and PSNR metrics were employed. The performance evaluation results obtained for different watermark sizes are presented in Table 1.

When the values presented in Table 2 are examined, it is observed that NC $\geq$ 0.97 is achieved for different cover images and watermark sizes. The BER values are very close to zero (with a maximum BER of 0.0070), indicating that the watermark can be extracted with a negligible level of error. These results demonstrate that the proposed method provides high watermark extractability across different cover images and watermark sizes. Moreover, the high NC and low BER values obtained particularly for medical images further support the suitability of the proposed method for applications involving sensitive data.

Secondly, when evaluated in terms of watermark size, a clear increase in PSNR values is observed as the watermark size decreases. The fact that all obtained PSNR values are above 37 dB, which is widely accepted in the literature as the threshold for high perceptual quality and imperceptibility, indicates that the proposed method achieves satisfactory imperceptibility performance. This result shows that smaller watermarks introduce less distortion to the cover image and confirms the effectiveness of the proposed approach in terms of imperceptibility. An examination of the SSIM values reveals that they remain at approximately 0.999 throughout all experiments. Variations in either the cover image or the

Table 1 Optimized parameter values (k and α) for different watermark sizes and cover images

Cover Image	Watermark	Opt. k	Opt. α
Melanoma	256×256	182	0.0346
	128×128	80	0.0305
	64×64	42	0.0202
Cerebral	256×256	154	0.0173
	128×128	72	0.0183
	64×64	30	0.0284
Retinal Fundus	256×256	122	0.0077
	128×128	56	0.0137
	64×64	46	0.0229
Baboon	256×256	126	0.0090
	128×128	76	0.0120
	64×64	38	0.0115
Peppers	256×256	142	0.0206
	128×128	72	0.0181
	64×64	46	0.0219

Table 2 Performans evaluation for different watermark sizes

Cover Image	Watermark	NC	BER	PSNR	SSIM
Melanoma	256×256	0.9962	0.0006	37.042	0.9997
	128×128	0.9991	0.0022	44.064	0.9999
	64×64	0.9820	0.0034	51.440	0.9999
Cerebral	256×256	0.9994	0.0002	43.043	0.9994
	128×128	0.9990	0.0016	48.507	0.9998
	64×64	0.9962	0.0022	50.517	0.9999
Retinal Fundus	256×256	0.9893	0.0017	49.621	0.9996
	128×128	0.9964	0.0025	50.251	0.9997
	64×64	0.9963	0.0009	51.323	0.9998
Baboon	256×256	0.9983	0.0003	48.255	0.9999
	128×128	0.9923	0.0029	51.175	0.9999
	64×64	0.9700	0.0070	59.587	0.9999
Peppers	256×256	0.9995	0.0002	41.493	0.9996
	128×128	0.9979	0.0017	48.767	0.9999
	64×64	0.9964	0.0034	51.275	0.9999

watermark size do not lead to a significant decrease in SSIM values.

This finding indicates that the proposed method preserves not only pixel-level similarity but also the structural integrity of the image. Since maintaining structural integrity is of critical impor-

Table 3 NC Values obtained against different attacks (watermark: 64x64)

Type of Attacks	Noise Density	Retinal Fundus	Baboon	Peppers
No Attack	–	0.9963	0.9700	0.9964
Gaussian low-pass filter	3×3	0.9625	0.8089	0.9313
Median	3×3	0.9912	0.8978	0.9669
Rescaling	0.25–4	0.9486	0.8083	0.9337
Gaussian noise	0.001	0.9053	0.8809	0.8306
Salt and pepper noise	0.001	0.9180	0.9448	0.9727
Speckle noise	0.001	0.9797	0.9452	0.9767
JPEG compression	50	0.9323	0.8242	0.9503
JPEG2000 compression	12	0.9951	0.9072	0.9879
Sharpening attack	0.8	0.9575	0.8370	0.9203
Average filter	3×3	0.9626	0.8087	0.9404

tance in medical imaging applications, the obtained results further support the applicability of the proposed method to such sensitive use cases.

Table 3 presents the robustness evaluation of the proposed method against different types of attacks using Retinal Fundus, Baboon, and Peppers as cover images when the watermark size is fixed at 64×64. The robustness performance is assessed in terms of the NC metric.

The conducted attack analyses demonstrate that the proposed DWT–SVD-based watermarking method exhibits a high level of robustness against various attack types. Owing to its frequency-domain characteristics, the method successfully preserves NC values, particularly under JPEG2000 compression, speckle noise, and salt-and-pepper noise attacks. On the other hand, Gaussian noise and geometric rescaling attacks are observed to have a more limiting effect on performance, especially for images with high texture complexity, such as Baboon. Nevertheless, even under these challenging attack conditions, the obtained NC values remain at acceptable levels, indicating that the embedded watermark can still be reliably extracted.

Overall, the experimental results indicate that the proposed watermarking method achieves high robustness and imperceptibility across different cover images and watermark sizes. As the watermark size decreases, an improvement in perceptual image quality is observed. The fact that all obtained values remain above the thresholds commonly accepted in the literature confirms that the proposed approach provides a stable, reliable, and generalizable performance under a wide range of attack scenarios.

CONCLUSION

In this study, a hybrid digital watermarking method based on dimensionality reduction and optimization is proposed to ensure copyright protection and data security for both color and medical images. In the proposed approach, DWT and SVD are jointly applied only to the B channel of the color host image, while the watermark image is preprocessed through dimensionality reduction. The optimal embedding parameters are determined using the GWO algorithm. In this way, a balanced trade-off between imperceptibility and robustness is achieved.

Experimental studies were conducted on both standard test images and medical images under various watermark sizes and different attack scenarios. The obtained results demonstrate that the proposed method provides high imperceptibility under all test conditions. The fact that PSNR values remain above the threshold commonly accepted in the literature across all experiments, and that SSIM values are consistently around 0.999, indicates that the watermarking process has a negligible effect on image quality and structural integrity. This is particularly important for medical imaging applications, where preserving visual fidelity and structural information is critical. Robustness analyses reveal that the proposed method exhibits strong resistance against both classical signal processing attacks and compression- and noise-based attacks. The NC values obtained under different attack types are mostly above 0.90, confirming that the embedded watermark can be reliably extracted. In addition, BER values remaining close to zero clearly demonstrate the effectiveness of the frequency-domain-based structure of the method as well as the optimization process.

Furthermore, the analysis of optimized parameters for different watermark sizes shows that the use of fixed parameters may be insufficient in terms of performance. Thanks to the GWO-based optimization approach, the optimal rank value and embedding strength are automatically determined for each host image and watermark size, significantly enhancing the generalizability and adaptability of the method. The obtained findings support the importance of optimization-based approaches in improving the performance of digital watermarking systems. In conclusion, the proposed digital watermarking method offers high imperceptibility, strong robustness, and balanced performance characteristics. It provides an effective and reliable solution for application areas such as medical image security, copyright protection, and the prevention of unauthorized use of sensitive data. In future work, the proposed method will be evaluated in different color spaces (e.g., YCbCr, HSV), integrated with deep learning-based optimization approaches, and improved to reduce computational cost for real-time systems.

Ethical standard

The authors have no relevant financial or non-financial interests to disclose.

Availability of data and material

The data that support the findings of this study are available from the corresponding author upon reasonable request.

Conflicts of interest

The authors declare that there is no conflict of interest regarding the publication of this paper.

LITERATURE CITED

Agarwal, N. and P. K. Singh, 2022 Discrete cosine transforms and genetic algorithm based watermarking method for robustness and imperceptibility of color images for intelligent multimedia applications. Multimedia tools and applications **81**: 19751–19777.

Ahmadi, S. B. B., G. Zhang, M. Rabbani, L. Boukela, and H. Jelodar, 2021 An intelligent and blind dual color image watermarking for authentication and copyright protection. Applied Intelligence **51**: 1701–1732.

Anand, A. and A. K. Singh, 2021 Watermarking techniques for medical data authentication: a survey. Multimedia Tools and Applications **80**: 30165–30197.

Awasthi, D., A. Tiwari, P. Khare, and V. K. Srivastava, 2024 A comprehensive review on optimization-based image watermarking techniques for copyright protection. Expert Systems with Applications **242**: 122830.

Begum, M. and M. S. Uddin, 2020 Digital image watermarking techniques: a review. Information **11**: 110.

Çelik, H. and N. Doğan, 2021 K-en az anlamlı bitlere dayalı kaotik bir harita kullanan renkli görüntü steganografisi. Politeknik Dergisi **26**: 679–692.

Çelik, S. and N. Yalçın, 2023 Kriptografi ve görüntü steganografi tabanlı bir veri gizleme uygulaması: Sten 0.1. Bilgisayar Bilimleri ve Teknolojileri Dergisi **4**: 56–66.

Çetinkaya, Z. and F. Horasan, 2025 An optimized watermarking technique for medical images using dimension reduction. In *2025 9th International Symposium on Innovative Approaches in Smart Technologies (ISAS)*, pp. 1–6, IEEE.

Eltoukhy, M. M., A. E. Khedr, M. M. Abdel-Aziz, and K. M. Hosny, 2023 Robust watermarking method for securing color medical images using slant-svd-qft transforms and otp encryption. Alexandria Engineering Journal **78**: 517–529.

Gull, S. and S. A. Parah, 2024 Advances in medical image watermarking: a state of the art review. Multimedia Tools and Applications **83**: 1407–1447.

Horasan, F., H. Erbay, F. Varçın, and E. Deniz, 2019 Alternate low-rank matrix approximation in latent semantic analysis. Scientific Programming **2019**: 1095643.

Hu, H.-T., 2024 Synergistic compensation for rgb-based blind color image watermarking to withstand jpeg compression. Journal of Information Security and Applications **80**: 103673.

Karmouni, H., M. A. Tahiri, I. Dagal, H. Amakdouf, M. O. Jamil, *et al.*, 2024 Secure and optimized satellite image sharing based on chaotic eπ map and racah moments. Expert Systems with Applications **236**: 121247.

Khare, P. and V. K. Srivastava, 2021 A secured and robust medical image watermarking approach for protecting integrity of medical images. Transactions on Emerging Telecommunications Technologies **32**: e3918.

Li, Y., J. Li, U. A. Bhatti, J. Ma, D. Li, *et al.*, 2023 Robust zero-watermarking algorithm for medical images based on orb and dct. In *2023 26th ACIS International Winter Conference on Software Engineering, Artificial Intelligence, Networking and Parallel/Distributed Computing (SNPD-Winter)*, pp. 282–289, IEEE.

Mahto, D. K. and A. K. Singh, 2021 A survey of color image watermarking: State-of-the-art and research directions. Computers & Electrical Engineering **93**: 107255.

Mamuti, M., 2019 *Tibbi Görüntü Güvenliği İçin Yeni bir Sayisal Damgalama Yöntemi*. Master's thesis, Sakarya Universitesi (Turkey).

Melman, A. and O. Evsutin, 2023 Image data hiding schemes based on metaheuristic optimization: a review. Artificial Intelligence Review **56**: 15375–15447.

Mirjalili, S., 2015 How effective is the grey wolf optimizer in training multi-layer perceptrons. Applied intelligence **43**: 150–161.

Mohanarathinam, A., S. Kamalraj, G. Prasanna Venkatesan, R. V. Ravi, and C. Manikandababu, 2020 Retracted article: Digital watermarking techniques for image security: a review. Journal of Ambient Intelligence and Humanized Computing **11**: 3221–3229.

Mousavi, S. M., A. Naghsh, and S. Abu-Bakar, 2014 Watermarking techniques used in medical images: a survey. Journal of digital imaging **27**: 714–729.

Nawaz, S. A., J. Li, D. Li, M. U. Shoukat, U. A. Bhatti, *et al.*, 2025 Medical image zero watermarking algorithm based on dual-tree complex wavelet transform, alexnet and discrete cosine transform. Applied Soft Computing **169**: 112556.

Othman, G. and D. Q. Zeebaree, 2020 The applications of discrete wavelet transform in image processing: A review. Journal of Soft Computing and Data Mining **1**: 31–43.

Priyadarshini, P. and K. Naik, 2024 Privacy protection and authentication of electronic patient information using hashing and multi watermarking technique. Multimedia Tools and Applications **83**: 89893–89930.

Qasim, A. F., F. Meziane, and R. Aspin, 2018 Digital watermarking: Applicability for developing trust in medical imaging workflows state of the art review. Computer Science Review **27**: 45–60.

Rodríguez, L., O. Castillo, J. Soria, P. Melin, F. Valdez, *et al.*, 2017 A fuzzy hierarchical operator in the grey wolf optimizer algorithm. Applied Soft Computing **57**: 315–328.

Roy, S. and A. K. Pal, 2019 A hybrid domain color image watermarking based on dwt–svd. Iranian Journal of Science and Technology, Transactions of Electrical Engineering **43**: 201–217.

Sahir, M., T. Bekkouche, F. Belilita, and N. Amardjia, 2025 An optimized color image watermarking scheme based on hd and svd in dwt domain. Engineering, Technology & Applied Science Research **15**: 21639–21646.

Seyedali, M. and L. Andrew, 2014 Grey wolf optimizer advances engineering software. Elsevier .

Sharma, S., H. Sharma, J. B. Sharma, and R. C. Poonia, 2023 A secure and robust color image watermarking using nature-inspired intelligence. Neural Computing and Applications **35**: 4919–4937.

Sharma, S., J. J. Zou, G. Fang, P. Shukla, and W. Cai, 2024 A review of image watermarking for identity protection and verification. Multimedia Tools and Applications **83**: 31829–31891.

Singh, R., M. Saraswat, A. Ashok, H. Mittal, A. Tripathi, *et al.*, 2023 From classical to soft computing based watermarking techniques: A comprehensive review. Future Generation Computer Systems **141**: 738–754.

Su, Q. and B. Chen, 2018 Robust color image watermarking technique in the spatial domain. Soft Computing **22**: 91–106.

Su, Q., F. Hu, X. Tian, L. Su, and S. Cao, 2024 A fusion-domain intelligent blind color image watermarking scheme using graph-based transform. Optics & Laser Technology **177**: 111191.

Wang, D., F. Yang, and H. Zhang, 2016 Blind color image watermarking based on dwt and lu decomposition. Journal of Information Processing Systems **12**: 765–778.

Wang, G., T. Jiang, D. Zhang, and V. Vasil'ev, 2025 Color image watermarking scheme based on singular value decomposition of split quaternion matrices. Journal of the Franklin Institute **362**: 107508.

Wang, H., Z. Yuan, S. Chen, and Q. Su, 2023 Embedding color watermark image to color host image based on 2d-dct. Optik **274**: 170585.

Wang, X.-y., C.-p. Wang, H.-y. Yang, and P.-p. Niu, 2013 A robust blind color image watermarking in quaternion fourier transform domain. Journal of Systems and Software **86**: 255–277.

Yağcıoğlu, H. and A. Sondaş, 2021 Çoklu görsel nesnelere veri gizleme (steganografi). Kocaeli Üniversitesi Fen Bilimleri Dergisi **4**: 1–5.

Yurttakal, A. H. and F. Horasan, 2022 Kesik tekil değer ayrışımı ve ayrık dalgacık dönüşümü kullanılarak boyut indirgeme tabanlı dayanıklı dijital görüntü damgalama. Afyon Kocatepe Üniversitesi Fen Ve Mühendislik Bilimleri Dergisi **22**: 761–768.

Zainol, Z., J. S. Teh, M. Alawida, A. Alabdulatif, *et al.*, 2021 Hybrid svd-based image watermarking schemes: a review. IEEE Access **9**: 32931–32968.

How to cite this article: Özmen, İ., Çetinkaya, Z., Horasan, F., Varçın, F., and He, S. Adaptive–Scaled Digital Watermarking in Color Medical Imaging. *Computers and Electronics in Medicine*, 3(1), 99-108, 2026.